Negative Hydroxyl Ions for Breakdown in Liquid Water

Tanvir Farouk and Ali Aghdam

Re**A**cting **S**ystems & **A**dvanced **E**nergy **R**esearch
Department of Mechanical Engineering
University of South Carolina, Columbia, USA

MIPSE
International Online Plasma Seminar (IOPS)
August 19, 2021

Plasma discharge in liquids – Initiation

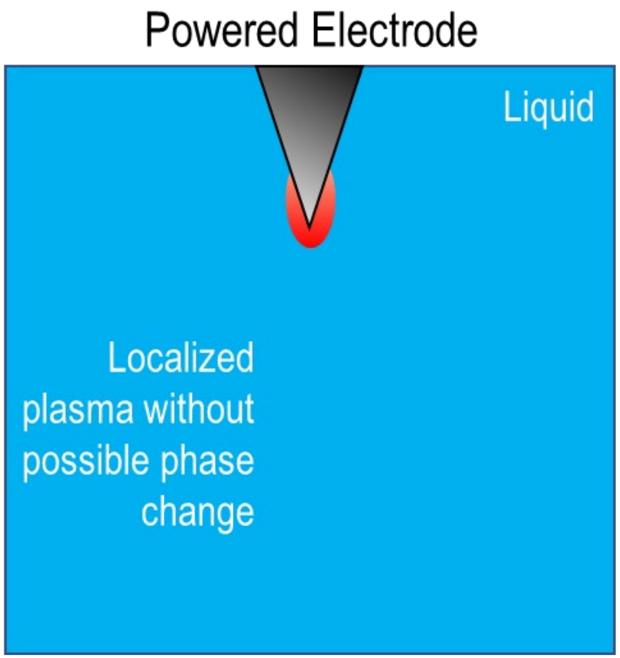

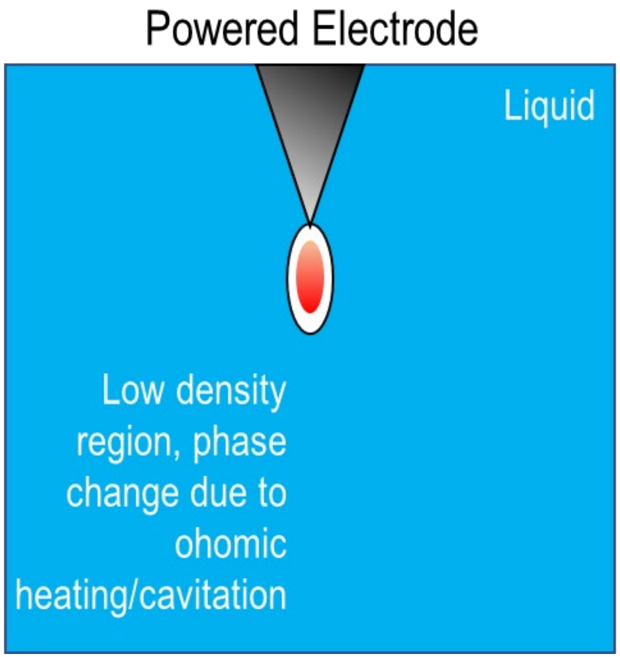

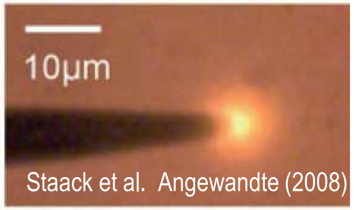

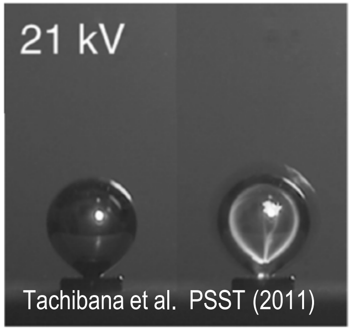

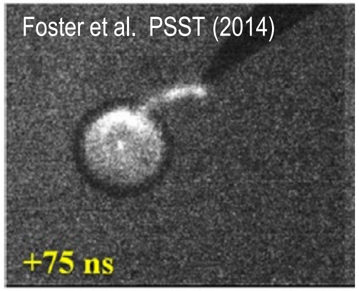

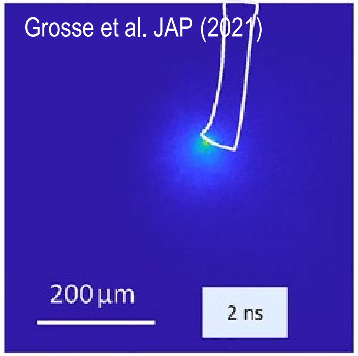

- Electron Multiplication Mechanism
  - Tunneling effect
- Multiphase Mechanism
  - Cavitation due to electric stress
  - Local ohmic heating
  - Formation of plasma in the bubble
  - Surface charge build-up at bubble surface

- Bruggeman and Leys, J. Phys. D: Appl. Phys. 42 (2009) 053001.
- Shneider et al., IEEE Trans. Dielectr. Electr. Insul., 19 (2012) 1579-1582.
- Bonaventura et al. PSST 30, (2021), 065023.
- Grosse et al. J. Appl. Phys. 129, (2021), 213302.

Plasma discharge in liquids – Initiation

- Electron Multiplication Mechanism

  - Tunneling effect (*Breakdown in transformer oils – extended to breakdown in water*)

Field dependent ionization of water molecule

$$Z_{H_2O_{aq}}(\mathbf{E}) = n_{H_2O_{aq}} \frac{q\,|\mathbf{E}|\,d}{h}\, exp\left(-\frac{m_e d \pi^2 \Delta^2}{q\,|\mathbf{E}|\,h^2}\right)$$

Δ = 4.00 eV

Tunneling detachment of electrons from OH[-*]

$$Z_{OH^-_{aq}}(\mathbf{E}) = n_{OH^-_{aq}} \frac{\pi A^2 q\,|\mathbf{E}|}{\sqrt{2 I_n m_e}}\, exp\left(-\frac{4}{3}\frac{\sqrt{2m_e}}{qh}\frac{I_n^{3/2}}{|\mathbf{E}|}\right)$$

I_n = 1.85 eV

- Probability of electron detachment from negative OH^-_{aq} is **greater than** the probability of field ionization of water molecules

- Detachment takes place at a **lower energy barrier**

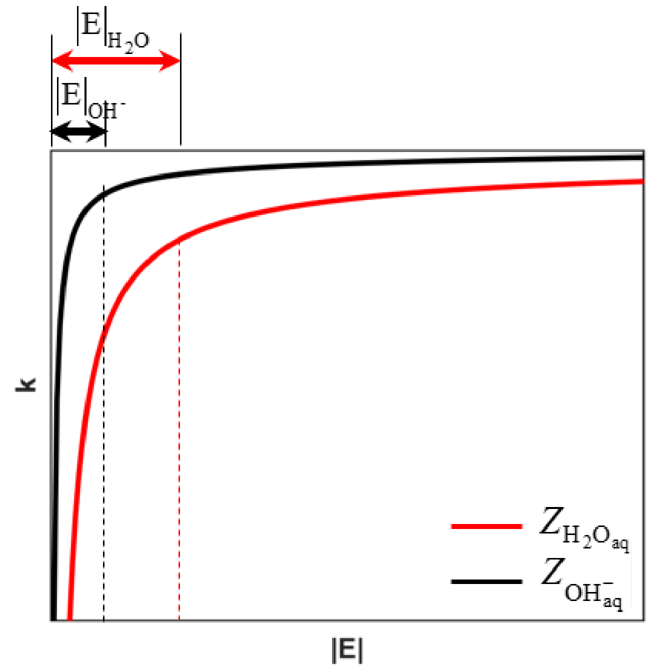

Schematic presentation and comparison of rate constants of field dependent ionization of H_2O_{aq} and tunneling detachment of electrons from OH^-_{aq} as a function of electric field magnitude.

*Shneider M, Pekker M, Liquid Dielectrics in an Inhomogeneous Pulsed Electric Field, Bristol, UK, 2016.
Joshi et al. J. Phys. D: Appl. Phys, 39, (2006), 359 – 369.

Plasma discharge in liquids – Initiation

- Electron Multiplication Mechanism
  - Tunneling effect (*Breakdown in transformer oils – extended to breakdown in water*)

Field dependent ionization of water molecule

$$Z_{H_2O_{aq}}(\mathbf{E}) = n_{H_2O_{aq}} \frac{q\,|\mathbf{E}|\,d}{h} exp\left(-\frac{m_e d \pi^2 \Delta^2}{q\,|\mathbf{E}|\,h^2}\right)$$

Δ = 4.00 eV

Tunneling detachment of electrons from OH-*

$$Z_{OH^-_{aq}}(\mathbf{E}) = n_{OH^-_{aq}} \frac{\pi A^2 q\,|\mathbf{E}|}{\sqrt{2 I_n m_e}} exp\left(-\frac{4}{3}\frac{\sqrt{2m_e}}{qh}\frac{I_n^{3/2}}{|\mathbf{E}|}\right)$$

I_n = 1.85 eV

Is there sufficient OH^-_{aq} present in water?

$$H_2O_{aq} \rightleftharpoons H^+_{aq} + OH^-_{aq}$$

$$n_{H^+_{aq}} = n_{OH^-_{aq}} = 6\times10^{19}\, m^{-3}$$

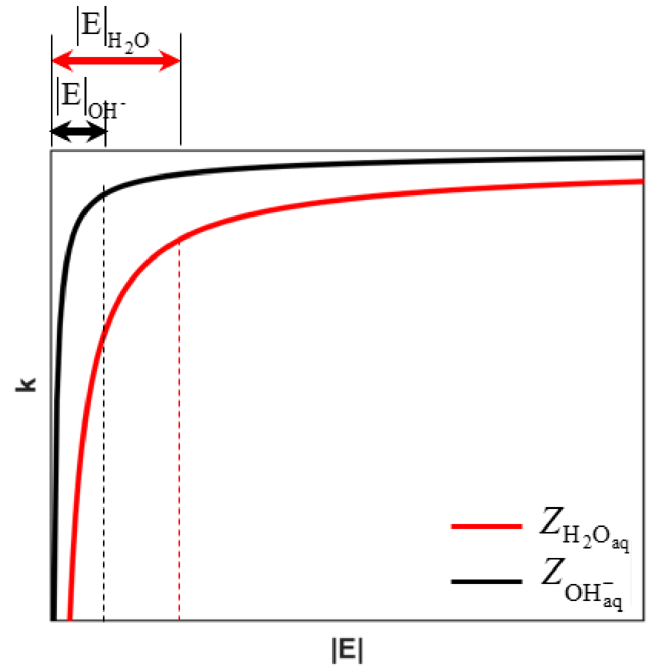

Schematic presentation and comparison of rate constants of field dependent ionization of H_2O_{aq} and tunneling detachment of electrons from OH^-_{aq} as a function of electric field magnitude.

*Shneider M, Pekker M, Liquid Dielectrics in an Inhomogeneous Pulsed Electric Field, Bristol, UK, 2016.
Joshi et al. J. Phys. D: Appl. Phys, 39, (2006), 359 – 369.

UofSC

Mathematical model

Fluid Model

- Continuity: $\frac{\partial \rho}{\partial t} + \nabla.(\rho \mathbf{U}) = 0$
- Momentum: $\frac{\partial \rho \mathbf{U}}{\partial t} + \nabla.(\rho \mathbf{U}\mathbf{U}) = \mu \nabla^2 \mathbf{U} - \nabla p + \mathbf{F}$
- Energy: $\frac{\partial \rho \boldsymbol{E}_{\mathbf{tot}}}{\partial t} + \nabla.(\rho \mathbf{U} \boldsymbol{E}_{\mathbf{tot}}) + \nabla.(p\mathbf{U}) = \nabla.(\Box.\mathbf{U}) - \nabla.q + \mathbf{J}_{\mathbf{ion}}.\mathbf{E}$
- Equation of state: $p = (p_o + B)\left(\frac{\rho}{\rho_0}\right)^{\gamma} - B$

Plasma Model

- Species: $\frac{\partial N_k}{\partial t} + \nabla.(Z_k \mu_k \mathbf{E}\, N_k) + \nabla.(\mathbf{U} N_k)$
  $= \nabla.(D_k \nabla N_e) + S_k \qquad k = e, n, p$
- Electric field: $\nabla.(\varepsilon \nabla \phi) = q_0 (N_p - N_n - N_e)$
  $\mathbf{E} = -\nabla \phi$
- Electric Force: $\mathbf{F} = q\mathbf{E} - \frac{\varepsilon_0}{2}\mathbf{E}^2 \nabla \varepsilon + \frac{\varepsilon_0}{2} \nabla \left(\mathbf{E}^2 \frac{\partial \varepsilon}{\partial \rho} \rho\right)$
- Permittivity model: $\frac{\partial \varepsilon}{\partial \rho}\rho \simeq a\varepsilon \quad , \quad \varepsilon = C\rho^{\alpha}$

Aghdam and Farouk, PSST, 29, (2020), 025011
Aghdam and Farouk, PSST 30, (2021), 065025

Mathematical model

Fluid Model

- Continuity: $\frac{\partial \rho}{\partial t} + \nabla.(\rho \mathbf{U}) = 0$
- Momentum: $\frac{\partial \rho \mathbf{U}}{\partial t} + \nabla.(\rho \mathbf{U}\mathbf{U}) = \mu \nabla^2 \mathbf{U} - \nabla p + \mathbf{F}$
- Energy: $\frac{\partial \rho E_{\mathrm{tot}}}{\partial t} + \nabla.(\rho \mathbf{U} E_{\mathrm{tot}}) + \nabla.(p\mathbf{U}) = \nabla.(\square.\mathbf{U}) - \nabla.q + \mathbf{J}_{\mathbf{ion}}.\mathbf{E}$

$$\mathbf{F} = q\mathbf{E} - \frac{\varepsilon_0}{2}\mathbf{E}^2 \nabla \varepsilon + \frac{\varepsilon_0}{2} \nabla \left(\mathbf{E}^2 \frac{\partial \varepsilon}{\partial \rho} \rho \right)$$

Force due to free charges and electric field (Electrostatic force)

Force due to inhomogeneous dielectric (Polarization force)

Electrostrictive forces due to non-uniform electric field (Ponderomotive force)

Aghdam and Farouk, PSST, 29, (2020), 025011
Aghdam and Farouk, PSST 30, (2021), 065025

Reaction kinetics

Table 1. Different species considered in the model[a].

Electrons	e, e_{aq}
Ions	H^+, H^-, OH^-, O^-, H_2O^+, OH^-_{aq}, O^-_{aq}, $O^-_{2,aq}$, $O^-_{3,aq}$, $H_2O^+_{aq}$, $HO^-_{2,aq}$, $H_3O^+_{aq}$
Neutrals	H, H_2, OH, H_{aq}, $H_{2,aq}$, OH_{aq}, O_{aq}, $O_{2,aq}$, $O_{3,aq}$, H_2O_{aq}, $HO_{2,aq}$, $H_2O_{2,aq}$

[a] *aq*: aqueous.

Table 2. The water reaction mechanism

#	Reaction	Rate
R1	$H_2O_{aq} \rightarrow H_2O^+ + e$	$Z_{H_2O}(\lvert\mathbf{E}\rvert)$
R2	$OH^-_{aq} \rightarrow OH + e$	$Z_{OH}(\lvert\mathbf{E}\rvert)$
R3	$e + H_2O_{aq} \rightarrow OH^- + H$	$f(\lvert\mathbf{E}\rvert/N)$
R4	$e + H_2O_{aq} \rightarrow H_2 + O^-$	$f(\lvert\mathbf{E}\rvert/N)$
R5	$e + H_2O_{aq} \rightarrow OH + H^-$	$f(\lvert\mathbf{E}\rvert/N)$
R6	$e + H_2O_{aq} \rightarrow H_2O^+ + 2e$	$f(\lvert\mathbf{E}\rvert/N)$
R7	$H_2O^+ + e \rightarrow H_2O_{aq}$	1.0×10^{-19}
R8	$e + H_2O_{aq} \rightarrow e_{aq} + H_2O_{aq}$	3.3×10^{-18}
R9	$H + H_2O_{aq} \rightarrow H_{aq} + H_2O_{aq}$	5.0×10^{-21}
R10	$H_2 + H_2O_{aq} \rightarrow H_{2,aq} + H_2O_{aq}$	5.0×10^{-21}
R11	$O^- + H_2O_{aq} \rightarrow O^-_{aq} + H_2O_{aq}$	5.0×10^{-21}
R12	$OH + H_2O_{aq} \rightarrow OH_{aq} + H_2O_{aq}$	5.0×10^{-21}
R13	$H^+ + H_2O_{aq} \rightarrow H_3O^+_{aq}$	5.0×10^{-21}
R14	$OH^- + H_2O_{aq} \rightarrow OH^-_{aq} + H_2O_{aq}$	5.0×10^{-21}
R15	$H_2O^+ + H_2O_{aq} \rightarrow H_2O^+_{aq} + H_2O_{aq}$	5.0×10^{-21}
R16	$e_{aq} + H_2O_{aq} \rightarrow H_{aq} + OH^-_{aq}$	3.2×10^{-26}
R17	$e_{aq} + H_2O^+_{aq} \rightarrow H_{aq} + OH_{aq}$	1.0×10^{-15}
R18	$2e_{aq} + 2H_2O_{aq} \rightarrow H_{2,aq} + 2OH^-_{aq}$	9.1×10^{-18}
R19	$e_{aq} + H_{aq} + H_2O_{aq} \rightarrow H_{2aq} + OH^-_{aq}$	6.9×10^{-44}
R20	$e_{aq} + OH_{aq} \rightarrow OH^-_{aq}$	5.0×10^{-17}
R21	$e_{aq} + O^-_{aq} + H_2O_{aq} \rightarrow 2OH^-_{aq}$	6.1×10^{-44}
R22	$e_{aq} + H_3O^+_{aq} \rightarrow H_{aq} + H_2O_{aq}$	3.8×10^{-17}
R23	$e_{aq} + H_2O_{2,aq} \rightarrow OH_{aq} + OH^-_{aq}$	1.8×10^{-17}
R24	$e_{aq} + HO^-_{2,aq} + H_2O_{aq} \rightarrow OH_{aq} + 2OH^-_{aq}$	9.7×10^{-45}
R25	$e_{aq} + O_{2,aq} \rightarrow O^-_{2,aq}$	3.2×10^{-17}
R26	$e_{aq} + O_{aq} \rightarrow O^-_{aq}$	3.2×10^{-17}
R27	$H_{aq} + H_2O_{aq} \rightarrow H_{2,aq} + OH_{aq}$	1.7×10^{-26}
R28	$H_{aq} + H_{aq} \rightarrow H_{2,aq}$	1.2×10^{-17}
R29	$H_{aq} + OH_{aq} \rightarrow H_2O_{aq}$	1.2×10^{-17}
R30	$H_{aq} + OH^-_{aq} \rightarrow e_{aq} + H_2O_{aq}$	3.7×10^{-20}
R31	$H_{aq} + H_2O_{2,aq} \rightarrow OH_{aq} + H_2O_{aq}$	1.5×10^{-19}
R32	$H_{2,aq} + H_2O_{2,aq} \rightarrow H_{aq} + OH_{aq} + H_2O_{aq}$	1.0×10^{-20}
R33	$H_{aq} + O_{2,aq} \rightarrow HO_{2,aq}$	3.5×10^{-17}
R34	$H_{aq} + HO_{2,aq} \rightarrow H_2O_{2,aq}$	1.7×10^{-17}
R35	$O_{aq} + H_2O_{aq} \rightarrow 2OH_{aq}$	2.2×10^{-23}
R36	$O_{aq} + O_{2,aq} \rightarrow O_{3,aq}$	5.0×10^{-18}
R37	$OH_{aq} + OH_{aq} \rightarrow H_2O_{2,aq}$	9.1×10^{-18}
R38	$OH_{aq} + O^-_{aq} \rightarrow HO^-_{2,aq}$	3.3×10^{-17}
R39	$OH_{aq} + H_{2,aq} \rightarrow H_{aq} + H_2O_{aq}$	7.0×10^{-20}
R40	$OH_{aq} + OH^-_{aq} \rightarrow O^-_{aq} + H_2O_{aq}$	2.2×10^{-17}
R41	$OH_{aq} + HO_{2,aq} \rightarrow H_2O_{aq} + O_{2,aq}$	1.0×10^{-17}
R42	$OH_{aq} + O^-_{2,aq} \rightarrow OH^-_{aq} + O_{2,aq}$	1.3×10^{-17}
R43	$O^-_{aq} + H_2O_{aq} \rightarrow OH^-_{aq} + OH_{aq}$	3.0×10^{-21}
R44	$O^-_{aq} + H_{2,aq} \rightarrow OH^-_{aq} + H_{aq}$	1.3×10^{-19}
R45	$O^-_{aq} + H_2O_{2,aq} \rightarrow O^-_{2,aq} + H_2O_{aq}$	8.3×10^{-19}
R46	$O^-_{aq} + HO^-_{2,aq} \rightarrow O^-_{2,aq} + OH^-_{aq}$	6.6×10^{-19}
R47	$O^-_{aq} + O_{2,aq} \rightarrow O^-_{3,aq}$	6.0×10^{-18}
R48	$O^-_{aq} + O^-_{2,aq} + H_2O_{aq} \rightarrow 2OH^-_{aq} + O_{2,aq}$	1.7×10^{-45}
R49	$OH_{aq} + H_2O_{2,aq} \rightarrow H_2O_{aq} + HO_{2,aq}$	4.5×10^{-20}
R50	$OH_{aq} + HO^-_{2,aq} \rightarrow OH^-_{aq} + HO_{2,aq}$	1.2×10^{-17}
R51	$H_2O^+_{aq} + H_2O_{aq} \rightarrow H_3O^+_{aq} + OH_{aq}$	1.0×10^{-23}
R52	$H_3O^+_{aq} + OH^-_{aq} \rightarrow H_{aq} + OH_{aq} + H_2O_{aq}$	1.0×10^{-16}
R53	$HO_{2,aq} + H_2O_{aq} \rightarrow H_3O^+_{aq} + O^-_{2,aq}$	3.3×10^{-24}
R54	$H_3O^+_{aq} + O^-_{2,aq} \rightarrow HO_{2,aq} + H_2O_{aq}$	1.0×10^{-25}

Problem geometry

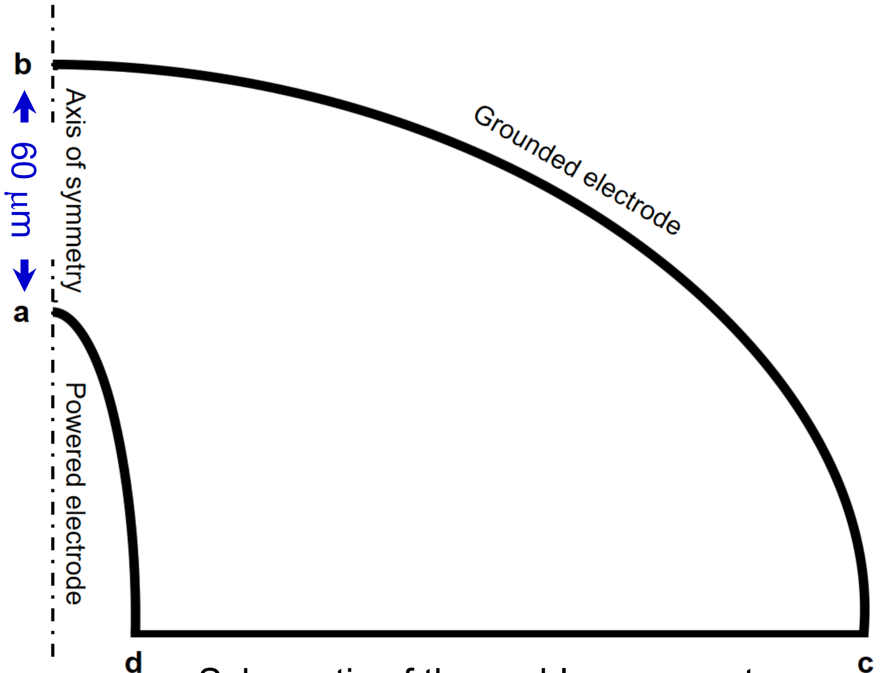

Schematic of the problem geometry

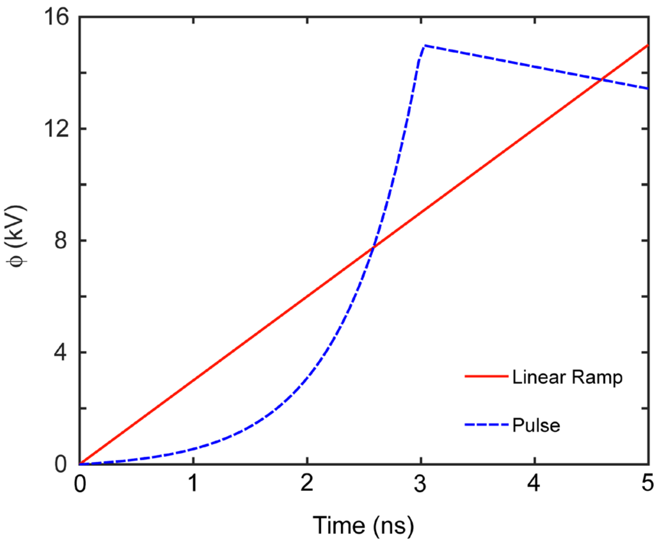

Transient voltage profile

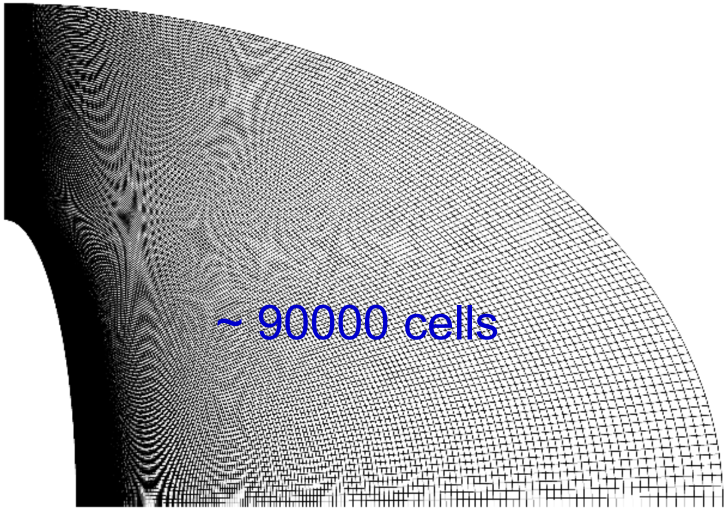

Case I: Electrons formed through ionization of water molecules via the Zener tunneling mechanism

Case II: Electrons formed through detachment from negative hydroxyl ions via tunneling mechanism

Case III: Electrons formed through a combination of ionization of water molecules and detachment from hydroxyl ions via the tunneling mechanism

Comparison of velocity field

Z_{H2O} | Z_{OH-} | Z_{H2O}, Z_{OH-}

Ramp

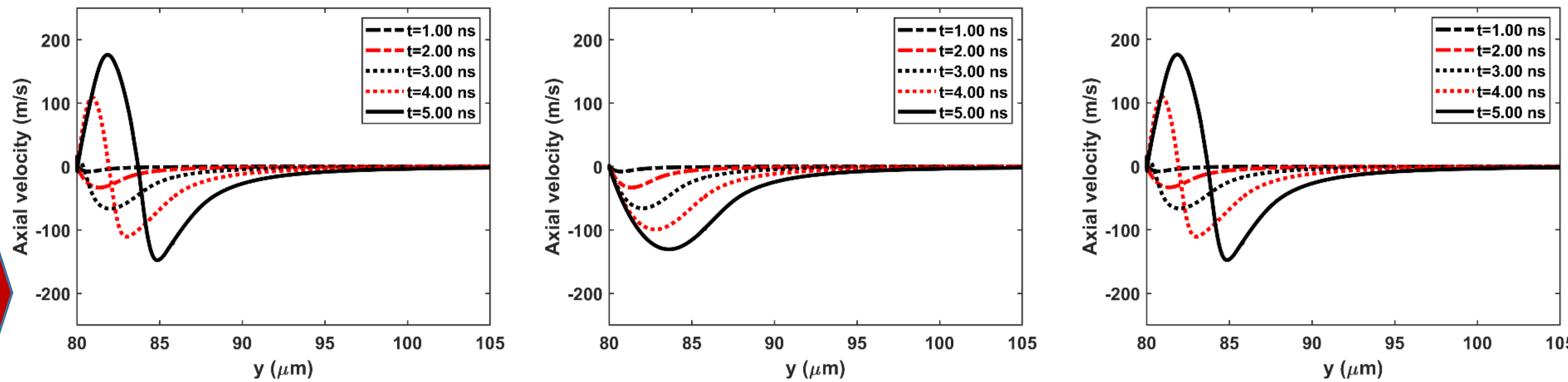

The positive velocity region does not appear for OH-, because the ionization degree is lower and less charges are produced.

Pulse

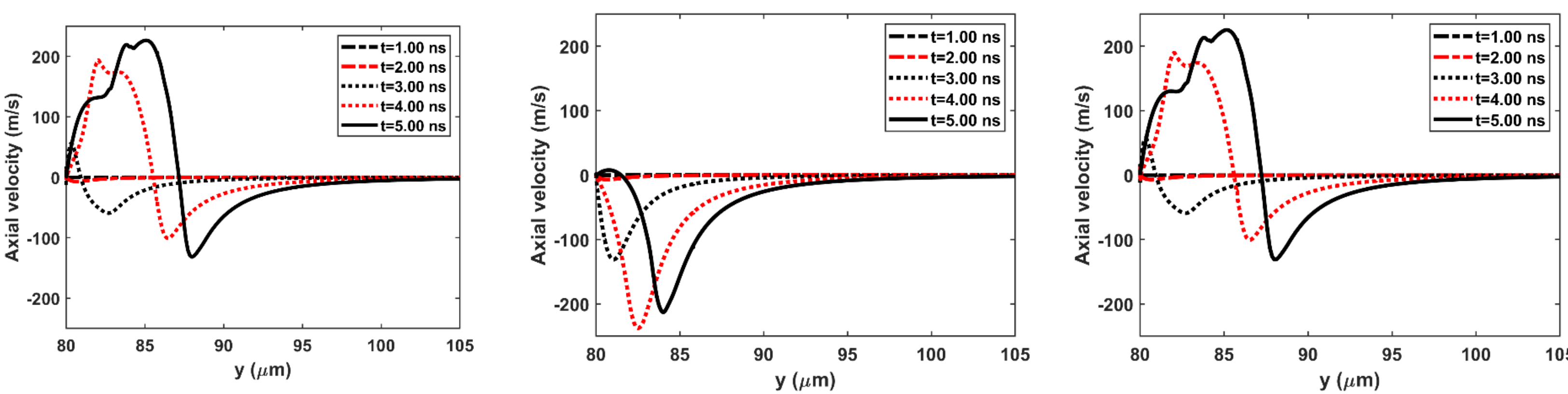

Comparison of density field

Z_{H2O} | Z_{OH-} | Z_{H2O}, Z_{OH-}

Ramp

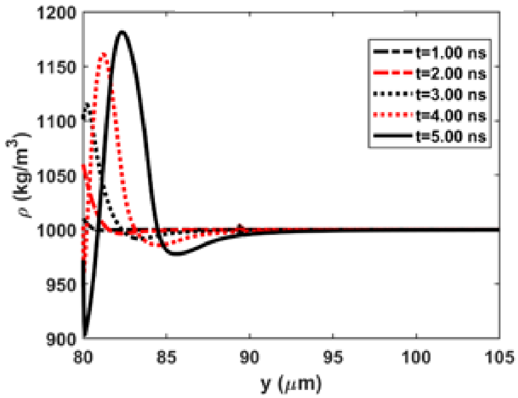

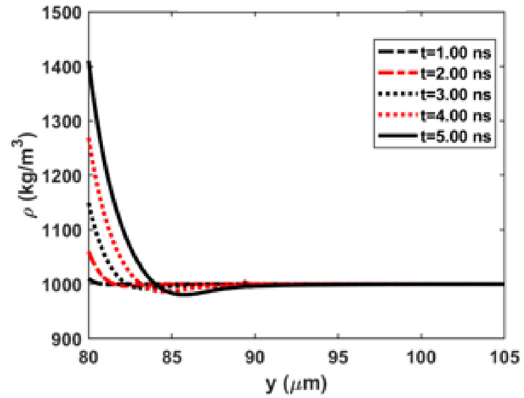

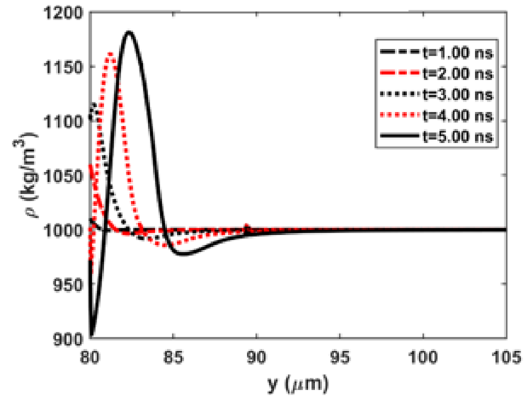

Compression and expansion regions. Sub-micron low density region. Tunnel detachment results in higher compression

Pulse

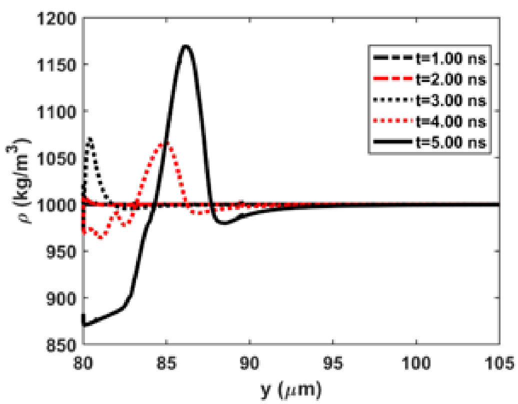

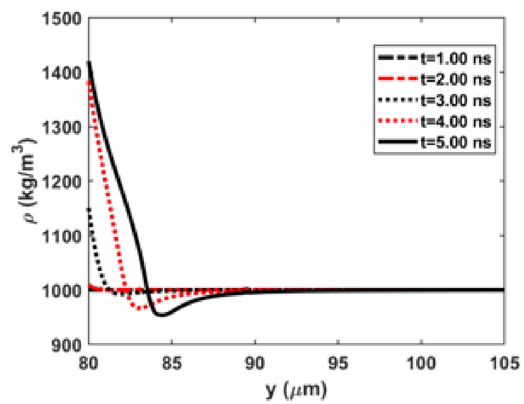

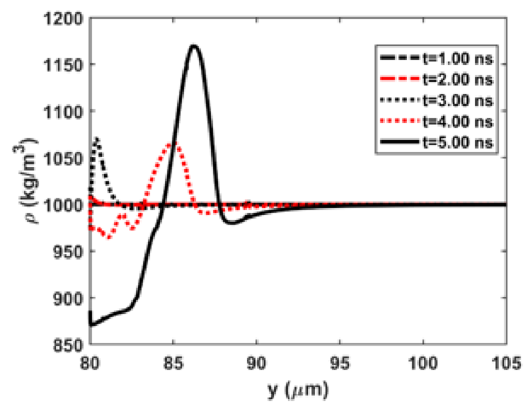

Comparison of electrical forces (Ramp)

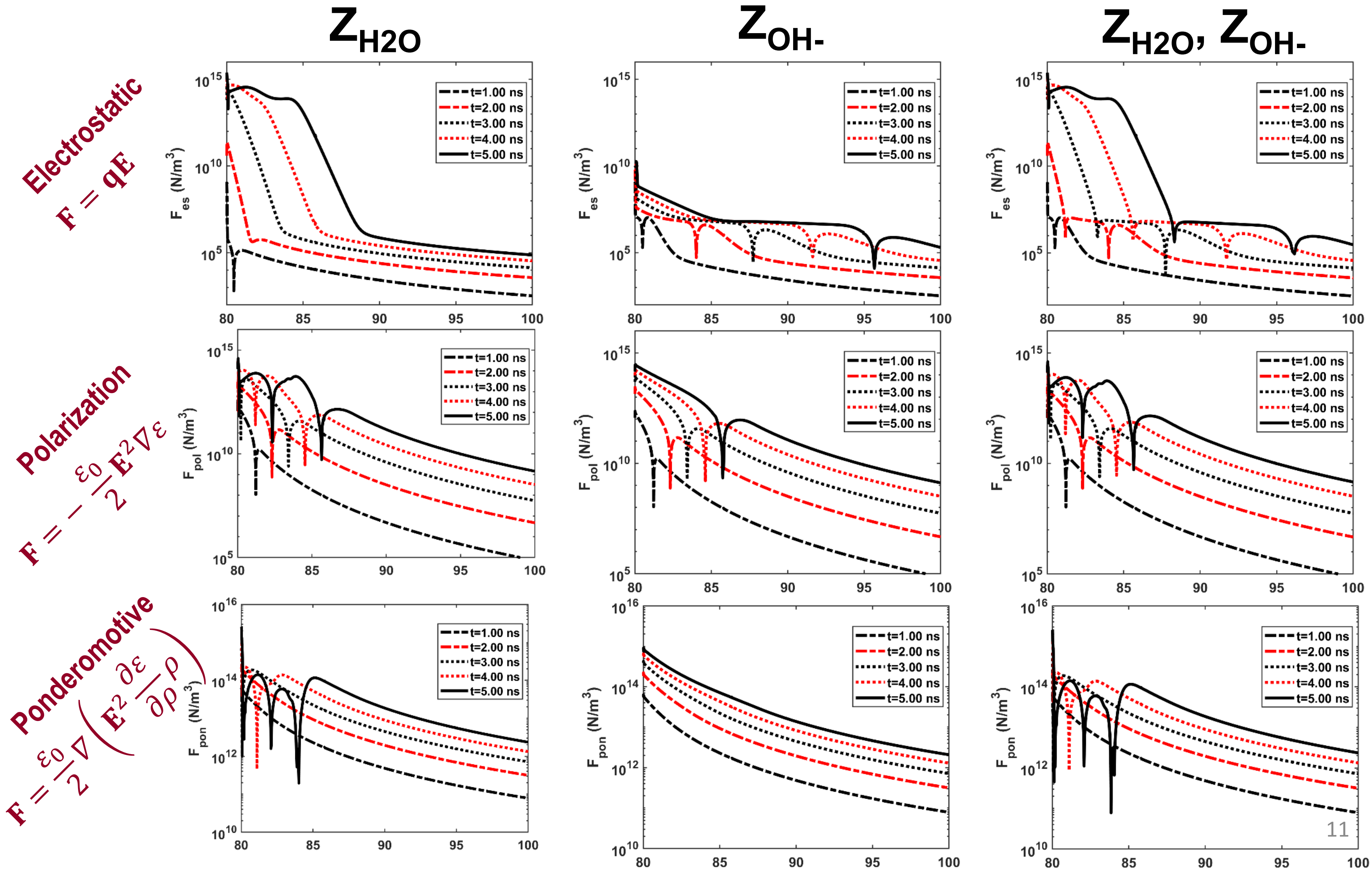

Comparison of electrons and OH^- number density (Ramp)

Z_{H2O} | Z_{OH-} | Z_{H2O}, Z_{OH-}

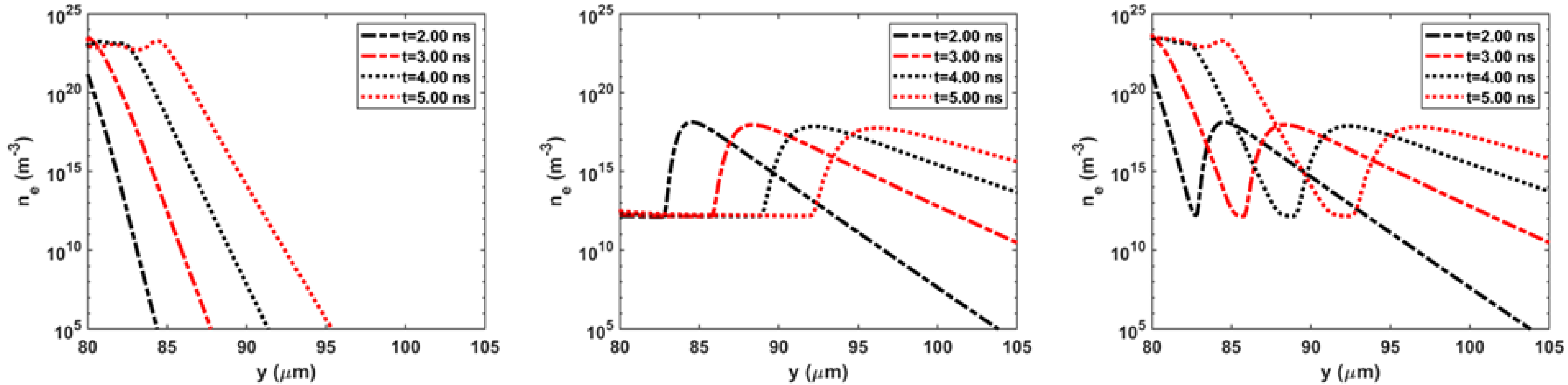

- OH^-_{aq} is rapidly consumed through the tunnel detachment process forming free electrons.
- Slow increase in the OH^-_{aq} due to solvated electrons and aqueous reactions.
- A strong and a weak wave

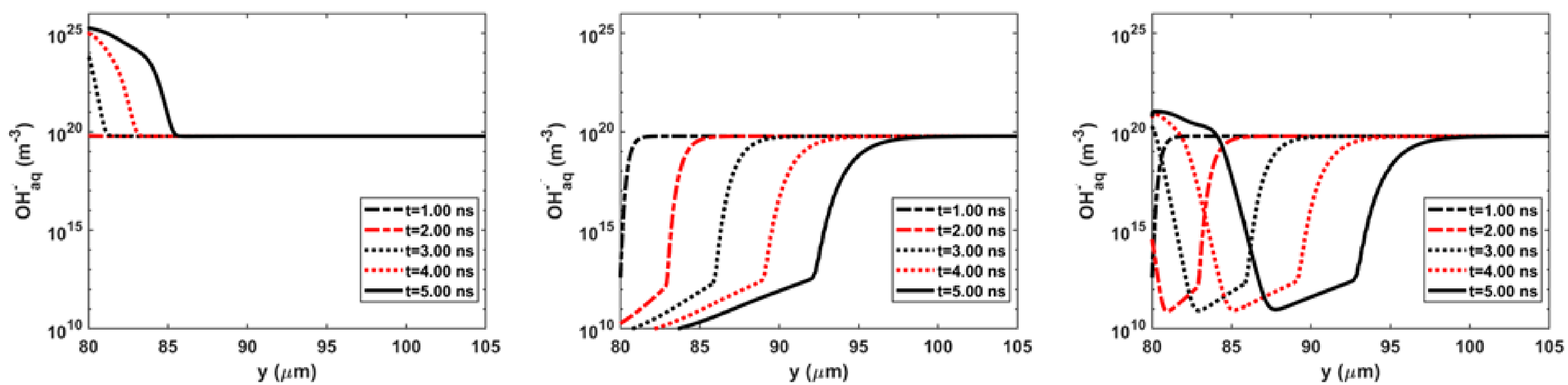

Comparison of electrons and OH^- number density (Pulse)

Z_{H2O} Z_{OH-} Z_{H2O}, Z_{OH-}

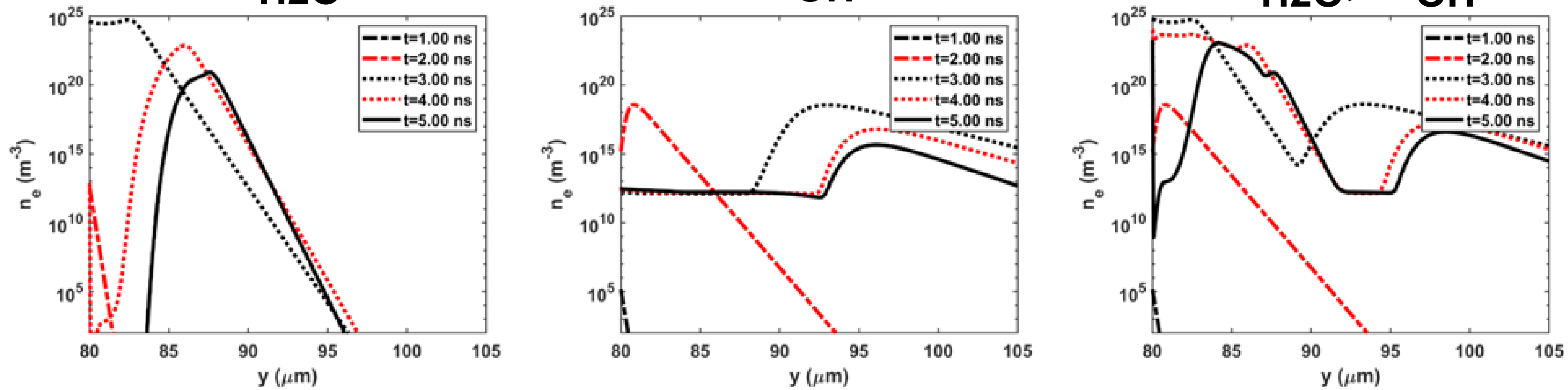

- OH^-_{aq} detachment has a longer delay for a pulse
- Higher concentration of OH^-_{aq} during replenishment

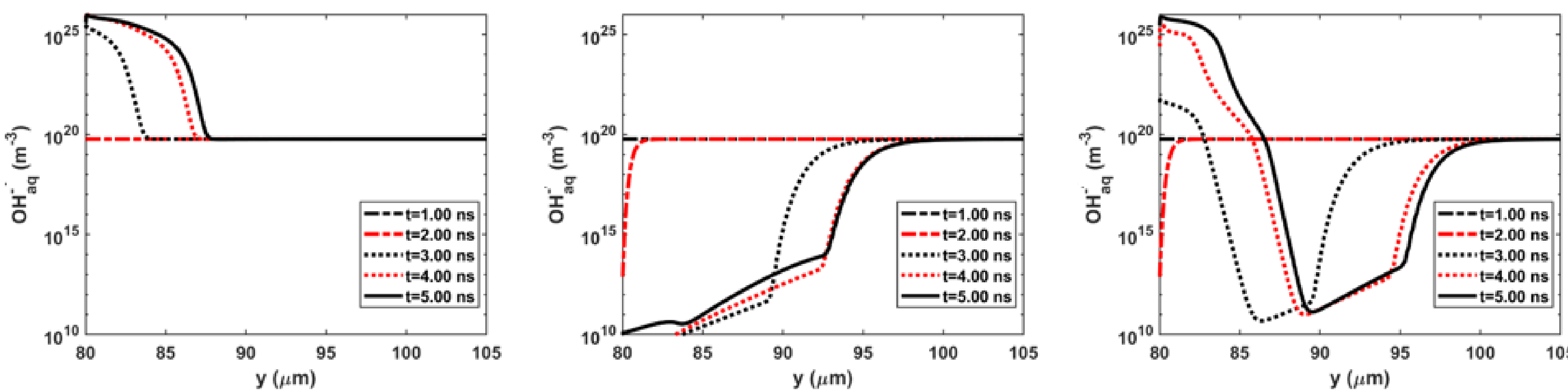

Spatiotemporal distribution of n_e and $n_{e,aq}$ ($Z_{H2O} + Z_{OH-}$, Ramp)

$$\text{R1. } H_2O_{aq} \rightarrow H_2O^+ + e$$
$$\text{R2. } OH^-_{aq} \rightarrow OH + e$$

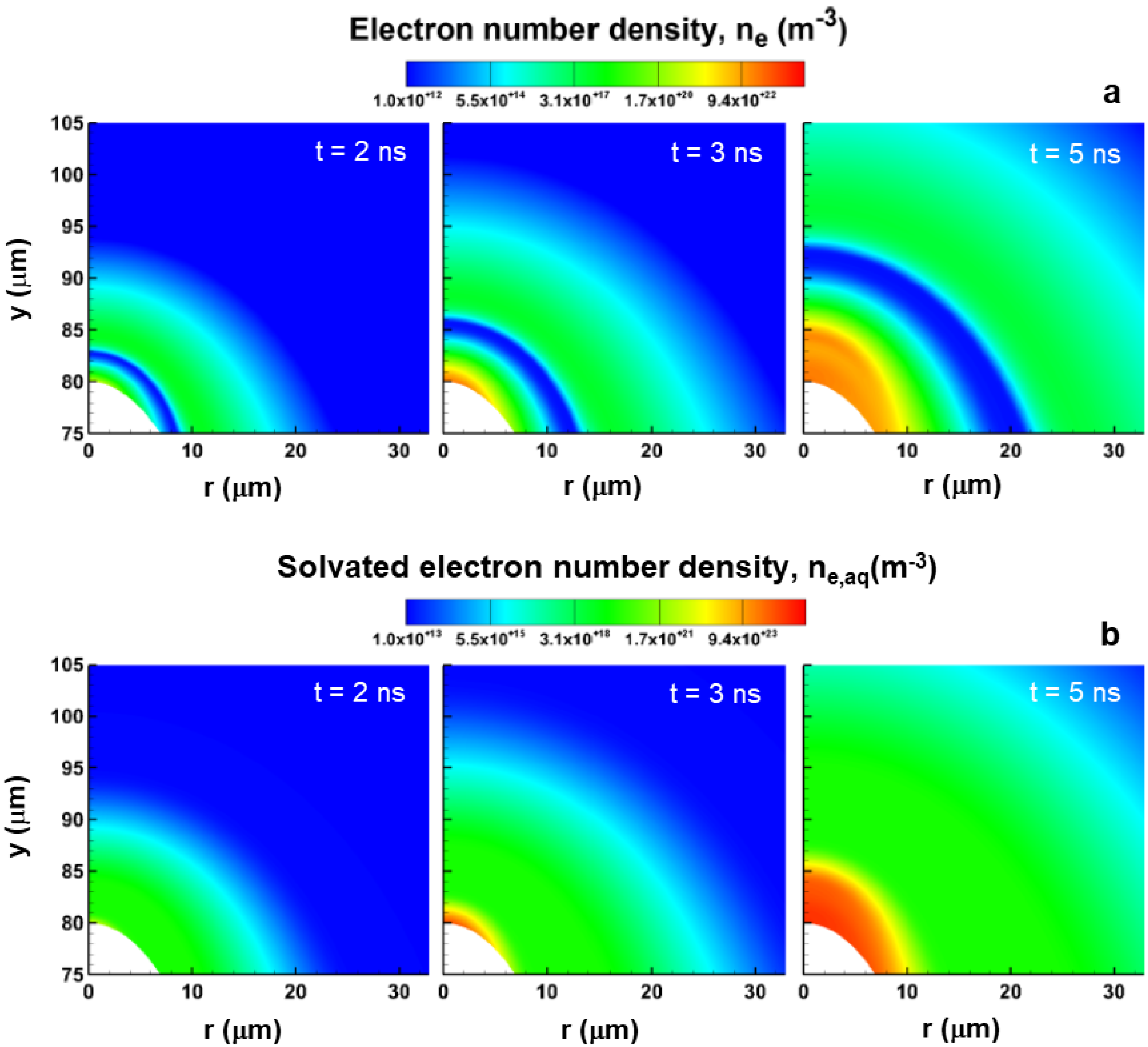

- First wave of electrons is formed through reaction R2 at earlier times and at lower driving voltage followed by a second ionization wave via R1 channel.
- R1 depends on the number density of H_2O_{aq}, which is multiple orders of magnitude higher than that of OH^-_{aq}.
- R1 channel rapidly surpasses the contribution from R2 once threshold energy is acquired.

Spatiotemporal distribution of n_e and $n_{e,aq}$ (Z_{H2O} + Z_{OH-}, Pulse)

R1. $H_2O_{aq} \rightarrow H_2O^+ + e$

R2. $OH^-_{aq} \rightarrow OH + e$

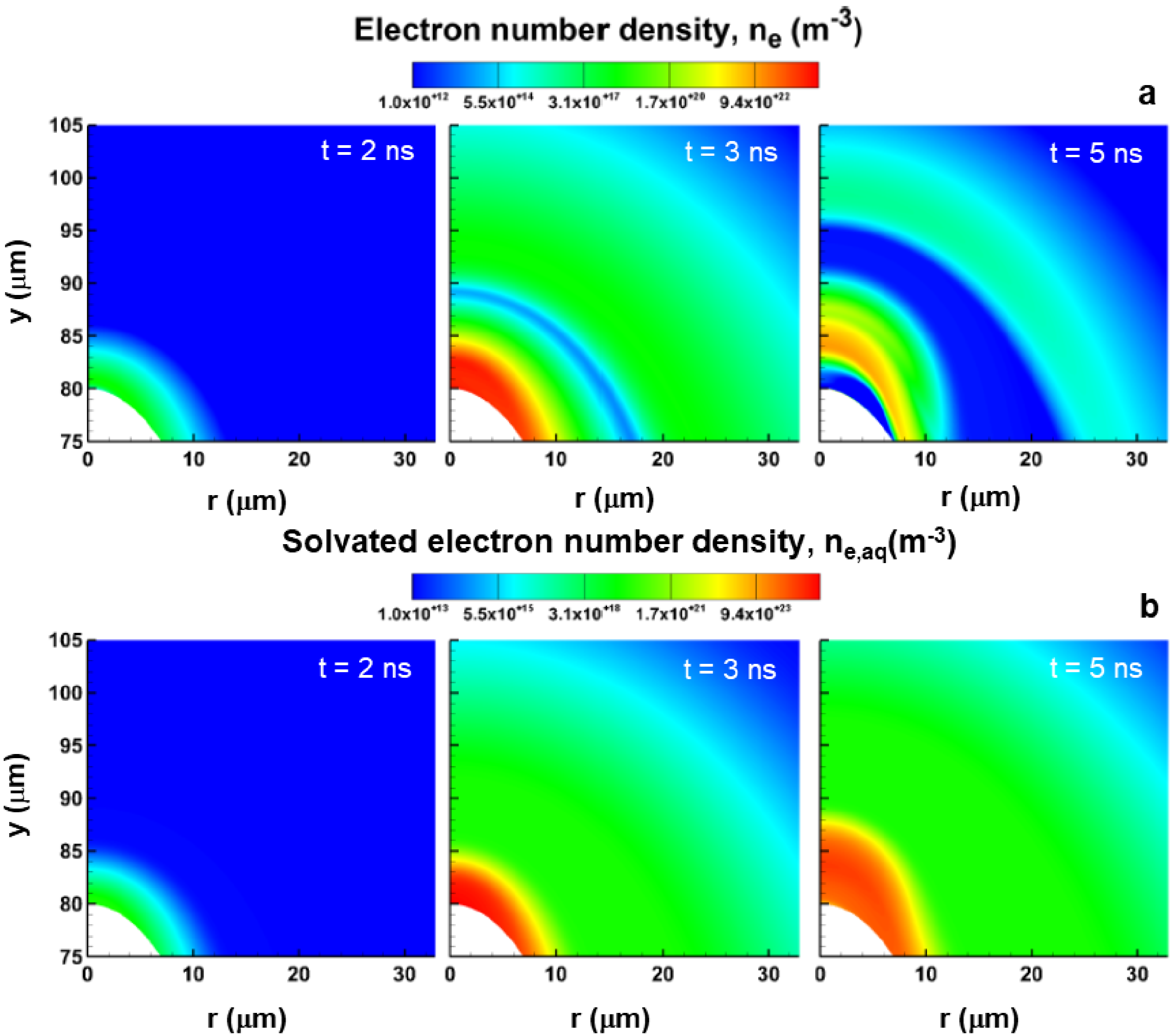

- The downstream advection occurs when the driving voltage starts the linear decay. The bulk fluid velocity attains the maximum value during the voltage relaxation period.
- Stratified regions of high density $n_{e,aq}$ due to the low mobility and diffusivity of the solvated electrons.

Spatiotemporal distribution of OH^-_{aq} and $H_3O^+_{aq}$

R1. $H_2O_{aq} \rightarrow H_2O^+ + e$

R2. $OH^-_{aq} \rightarrow OH + e$

- R2 channel becomes active once the depleted OH^-_{aq} is replenished near the vicinity of the powered electrode.
- Pulse profile generates charged species at higher concentration.

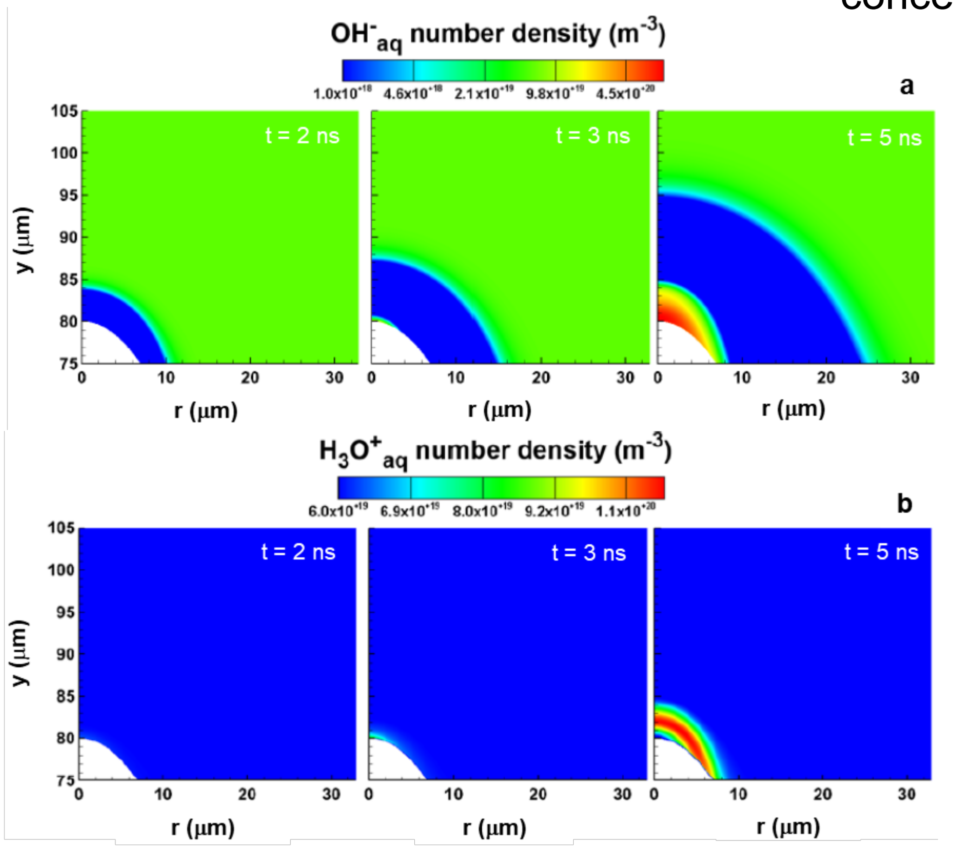

Ramp

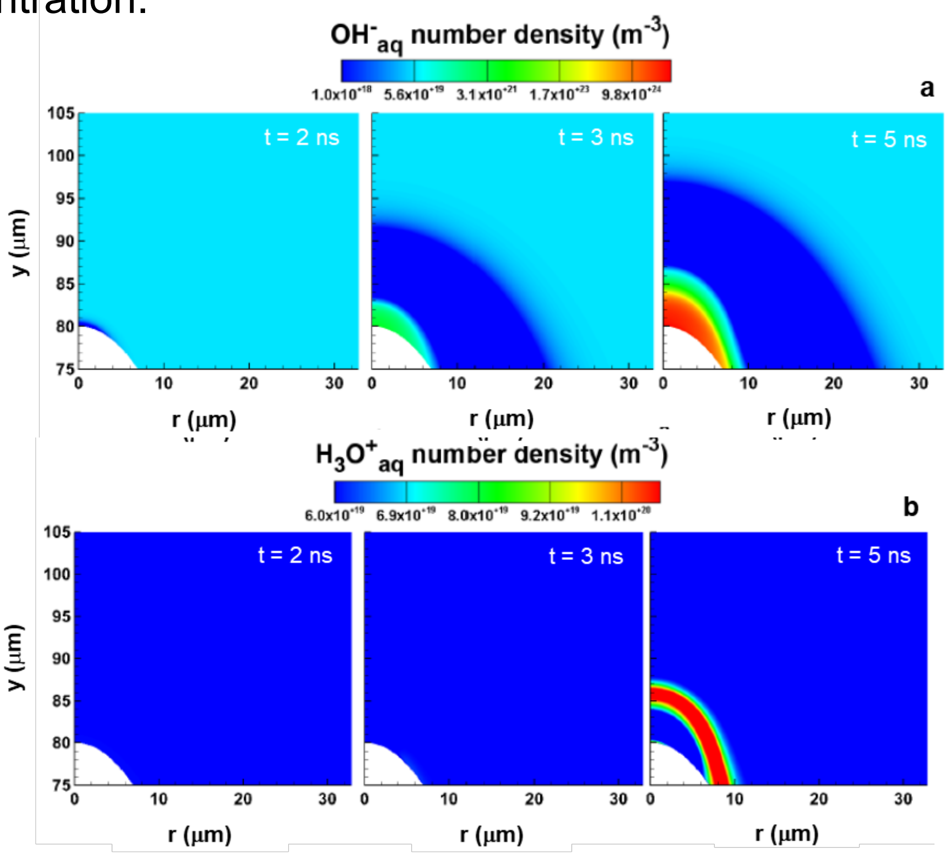

Pulse

Comparison of the reaction channels

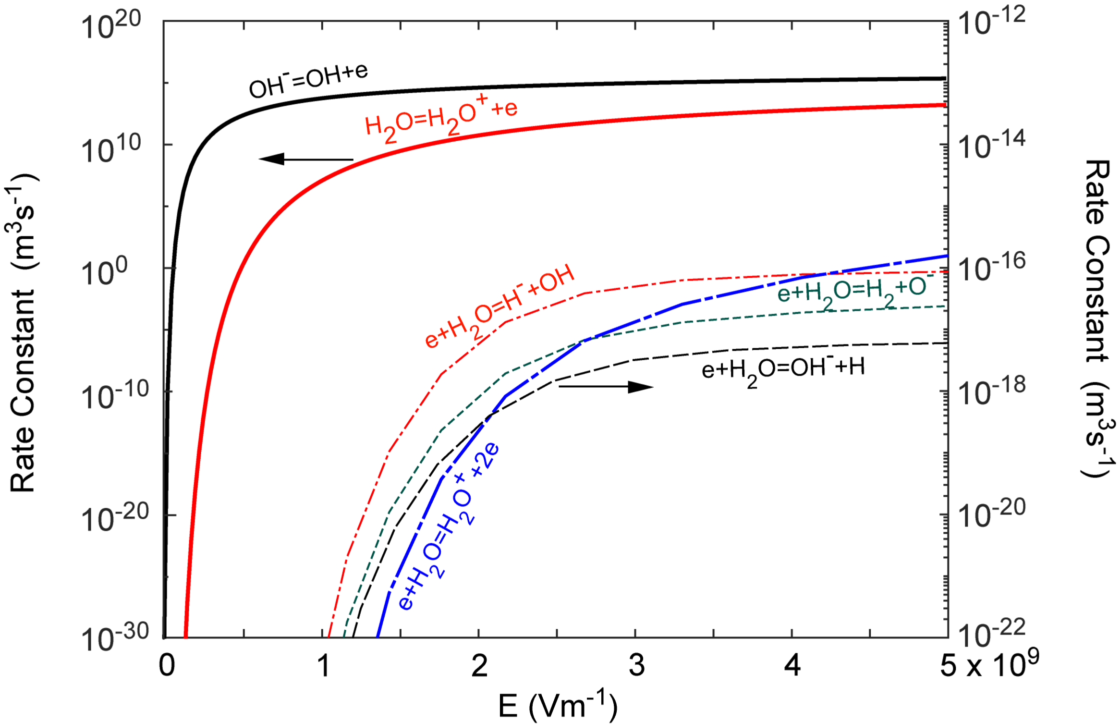

Reaction rate constants as function of electric field.

- Tunneling reactions supersedes all other electron impact reactions.

Comparison of the reaction channels

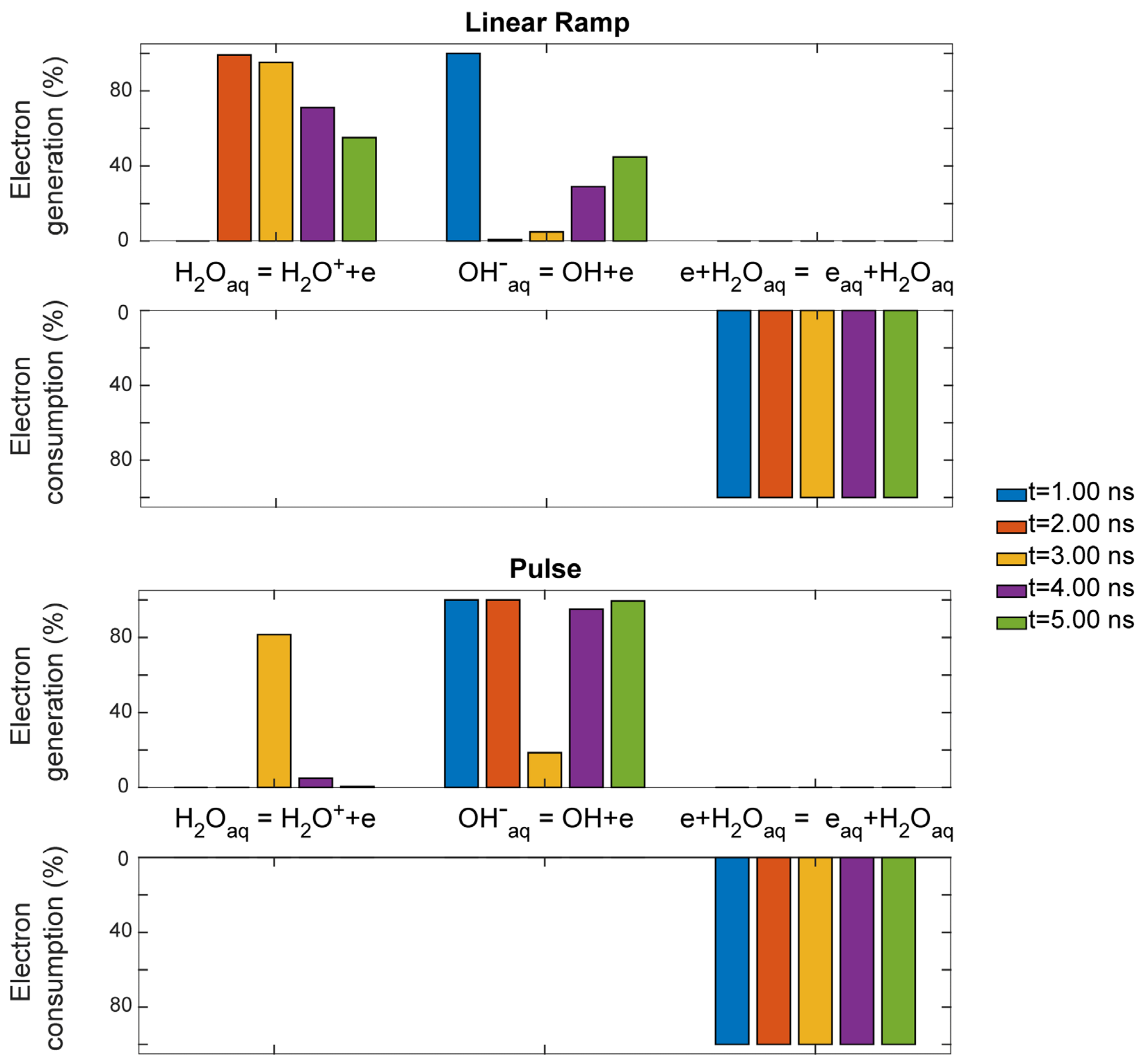

- During the voltage decay phase R1 diminishes drastically but R2 remains active.
- In a linear ramp after 2 ns, the contribution from R2 progressively builds up.
- As the OH^-_{aq} in the system gets replenished, the tunneling detachment remains as an active source for electrons.

Comparison of the reaction channels

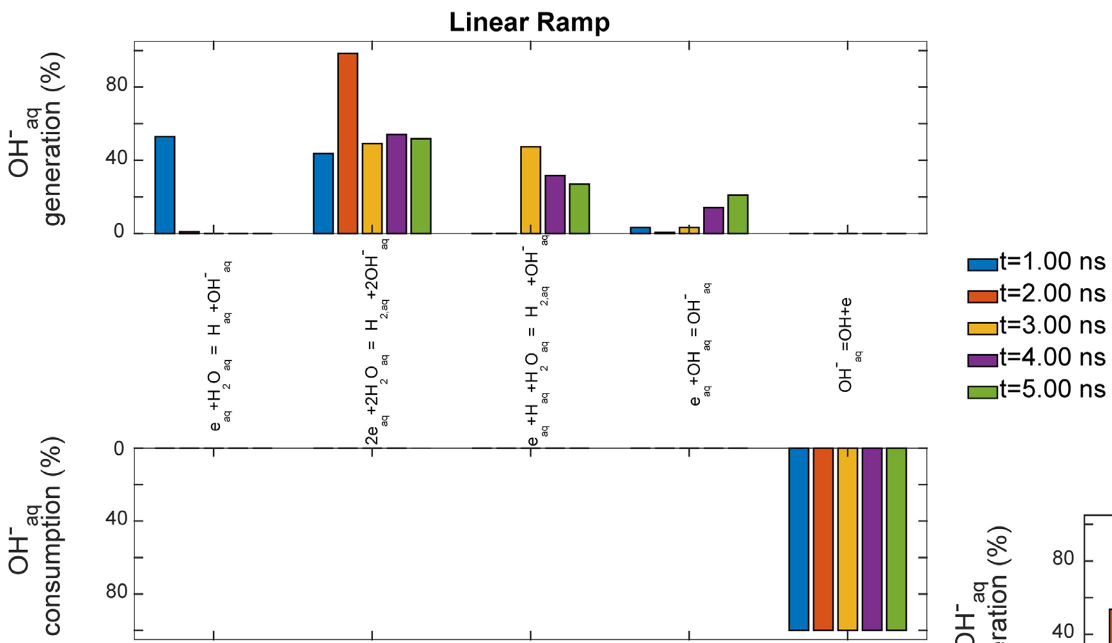

$$e_{aq} + H_2O_{aq} \rightarrow H_{aq} + OH^-_{aq}$$
$$2e_{aq} + 2H_2O_{aq} \rightarrow H_{2aq} + 2OH^-_{aq}$$
$$e_{aq} + H_{aq} + H_2O_{aq} \rightarrow H_{2aq} + OH^-_{aq}$$
$$e_{aq} + OH_{aq} \rightarrow OH^-_{aq}$$

Contribute to the formation of OH^-_{aq} in the system.

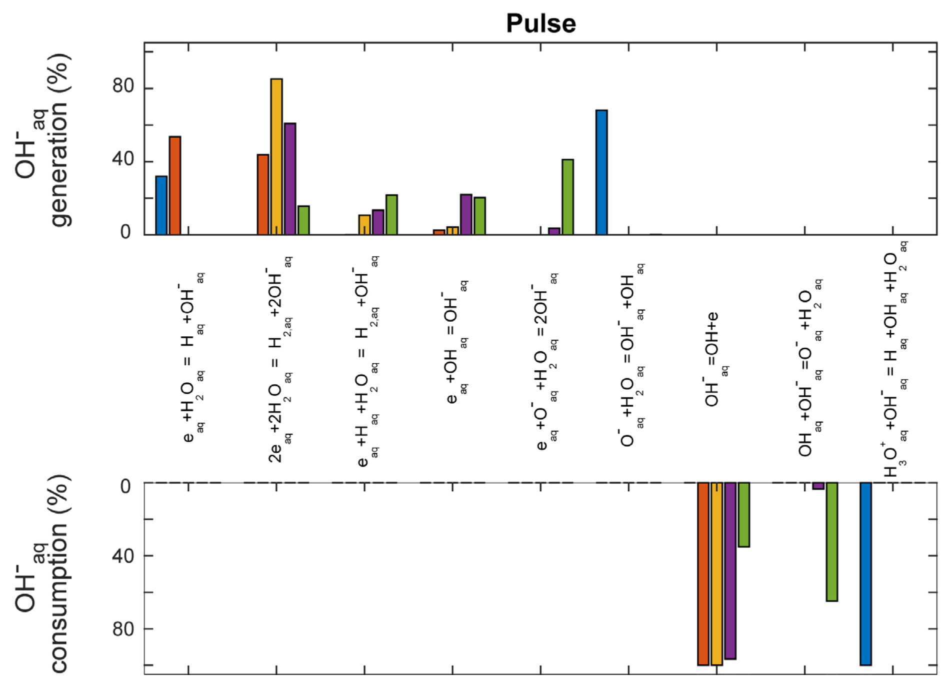

Summary

- Hydrodynamics associated with OH^-_{aq} detachment is distinctively different.
- The electrical forces from the tunnel detachment process generate stronger compression and weaker expansion regime.
- Majority of the electrons is produced from OH^-_{aq} ions during the pre-rise and the decay phase.
- The OH^-_{aq} in the system gets quickly depleted in regions where the detachment occurs and becomes a rate limiting condition.
- A strong and coupled recycling of OH^-_{aq} will allow both tunneling processes to remain active throughout the initiation process of the discharge.
- Tunneling from OH^-_{aq} does not decrease the density to the extent that is representative of nanovoids. The field ionization, which creates higher number of charged species can contribute to and enhance the cavitation of the liquid medium via the electrostatic force and augment nanovoid regions in the fluid

Acknowledgment

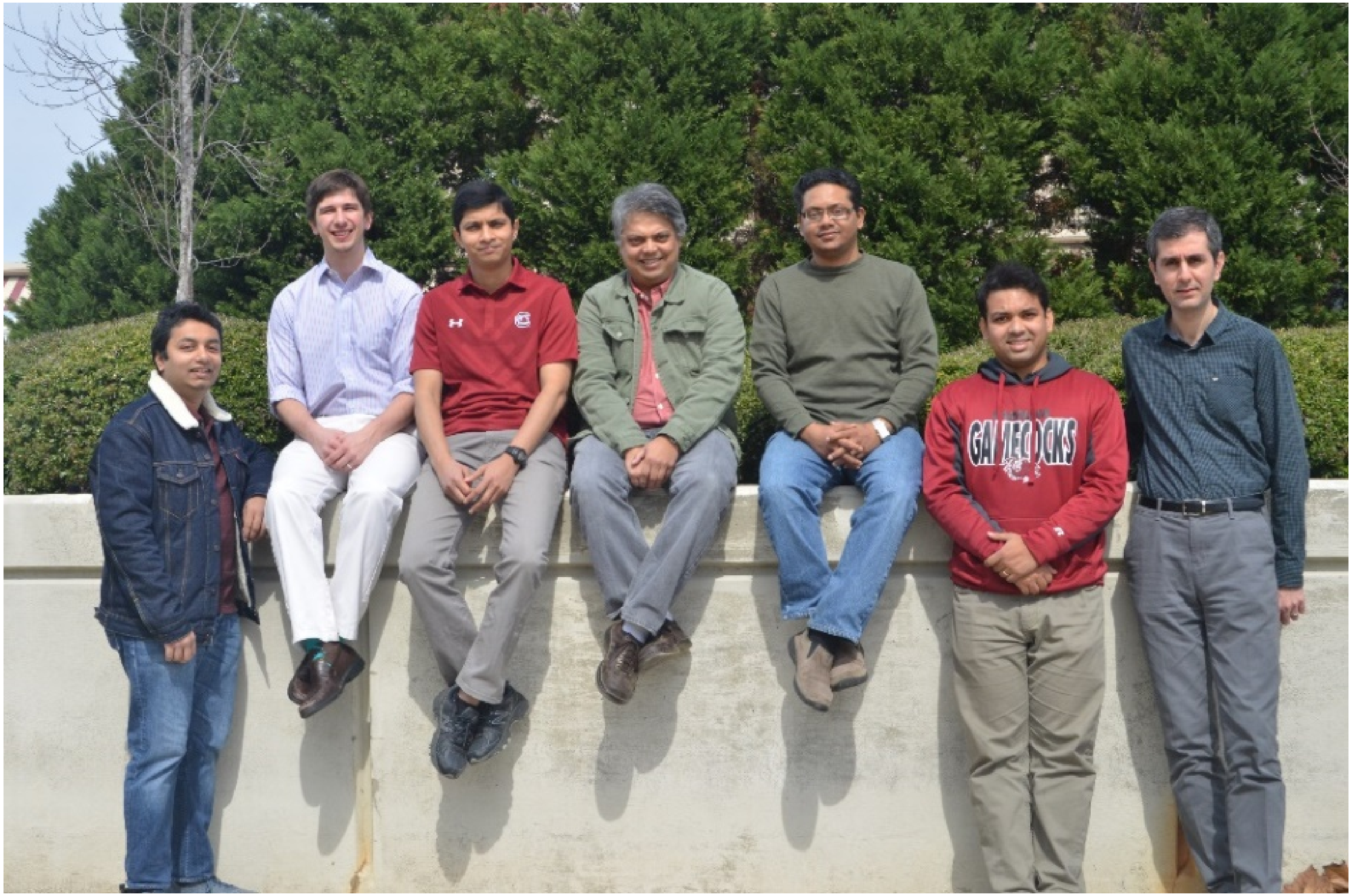

Division of Physics of the US National Science Foundation under Grant No. 1707282

Thank you!